PROCEEDINGS OF SCIENCE

Cosmology from EoR/Cosmic Dawn

Pritchard*†, Chang, Furlanetto, Choudhury, Zaroubi, Santos, Chen, Weller, Abdalla, Mesinger, Metcalf on behalf of the Cosmology-SWG and EoR/CD-SWG
Imperial College London
E-mail: j.pritchard@imperial.ac.uk

Robert Benton Metcalf
Dipartimento di Fisica e Astronomia, Universitá di Bologna, viale B. Pichat 6/2 , 40127, Bologna, Italy
E-mail: robertbenton.metcalf@unibo.it

Alkistis Pourtsidou
Dipartimento di Fisica e Astronomia, Universitá di Bologna, viale B. Pichat 6/2 , 40127, Bologna, Italy
E-mail: alkistis.pourtsidou@unibo.it

SKA Phase 1 will build upon early detections of the EoR by precursor instruments, such as MWA, PAPER, LOFAR, and HERA, to make the first high signal-to-noise measurements of fluctuations in the 21 cm brightness temperature from both reionization and the cosmic dawn. This will allow both imaging and statistical maps of the 21cm signal at redshifts $z = 6 - 30$ and constrain the underlying cosmology and evolution of the density field. This era includes nearly 60% of the (in principle) observable volume of the Universe and many more linear modes than the CMB, presenting an opportunity for SKA to usher in a new level of precision cosmology. This optimistic picture is complicated by the need to understand and remove the effect of astrophysics, so that systematics rather than statistics will limit constraints.

This chapter will describe the cosmological, as opposed to astrophysical, information available to SKA Phase 1. Key areas for discussion include: cosmological parameters constraints using 21cm fluctuations as a tracer of the density field; lensing of the 21cm signal, constraints on heating via exotic physics such as decaying or annihilating dark matter; impact of fundamental physics such as non-Gaussianity or warm dark matter on the source population; and constraints on the bulk flows arising from the decoupling of baryons and photons at $z = 1000$. The chapter will explore the path to separating cosmology from 'gastrophysics', for example via velocity space distortions and separation in redshift. We will discuss new opportunities for extracting cosmology made possible by the sensitivity of SKA-1 and explore the advances achievable with SKA-2.

Advancing Astrophysics with the Square Kilometre Array
June 8-13, 2014
Giardini Naxos, Italy

*Speaker.
†A footnote may follow.

1. Introduction

The years since the COBE observations of the CMB have ushered in an age of precision cosmology. Key cosmological parameters have been made possible by measurements of the distribution of matter in the Universe through WMAP and Planck observations of CMB anisotropies and large volume galaxy surveys such as SDSS. These surveys have made precision measurements of parameters describing the matter content of the Universe - the baryons Ω_b, dark matter Ω_c, dark energy Ω_Λ, radiation Ω_r, and neutrinos Ω_ν - and the physics of inflation - via the tilt n_s, amplitude A_s, running $\mathrm{d}n_s/\mathrm{d}\log k$ or the primordial potential power spectrum and r the ratio of tensor-to-scalar modes produced by inflation. These measurements have firmly established the basic picture of our Universe, known widely as the ΛCDM model of cosmology.

Despite this progress, measuring these numbers is only the first step towards a deep understanding of the underlying physics. Our ignorance of the nature of the dark matter and the dark energy or how neutrinos acquire mass and what value that mass takes are just two questions that modern cosmology hopes to address. Over the next decade two paths will help shed light on this. The simplest is simply to measure these cosmological parameters ever more precisely and over a wider range of times and scales in the hope of gaining further insights. The exemplar of this is with dark energy, where attempts to measure the redshift evolution of the dark energy density, parameterised by an equation of state $w(z)$, might distinguish a true cosmological constant from more general dark energy or modified gravity. For others there are critical thresholds of precision required to distinguish physical scenarios - for example, measuring the sum of the neutrino masses $M_\nu \lesssim 0.1$ would determine the neutrino mass hierarchy. Clearly more precision is a good thing, but it is not the only path forward.

Secondly, we can seek signatures of new physics in ways distinct from the distribution of large scale matter. The processes that produce dark matter will also allow it to annihilate and maybe to decay. The release of energy might have impact on the surrounding environment, heating the intergalactic medium. Pursuing unique signatures of new physics in new regimes will be a key part of the next decade.

The SKA is uniquely placed to probe cosmology as it is capable of mapping the Universe over wide volumes and an unprecedented range of redshifts. Figure 1 illustrates the additional range of volume and redshifts that the SKA will constrain. In this chapter, we will focus on the new opportunities created by SKA observations of the epoch of reionization (EoR) and the cosmic dawn (CD). This period has never before been observed offering a unique opportunity to test the consistency of the ΛCDM model and search for new hints to the great unanswered questions of cosmology.

[1]

2. Cosmological parameters from density fluctuations

Introduce fisher matrix formalism

In this section, we explore the ability of SKA to constrain cosmological parameters via observations of the density field. Just as galaxy surveys constrain cosmology by using galaxies as a tracer of the linear density field, SKA can constrain cosmology by using the 21 cm brightness

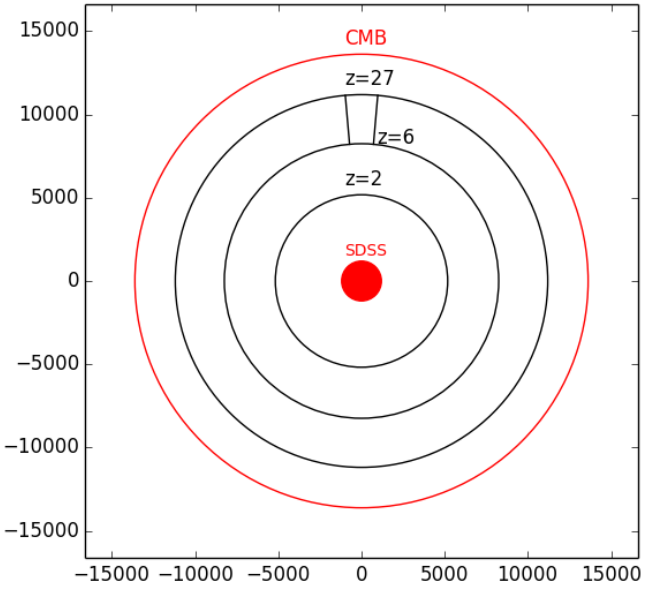

Figure 1: Illustration of the volume probed by SKA

temperature as a tracer of the density field. This is not an unproblematic assertion, since brightness temperature fluctuations may be sourced by variation in the spin temperature and neutral fraction in addition to the density field.

$$\delta T_B = (1+\delta)x_H ... \tag{2.1}$$

Equation 2.1 shows how these different terms come into play. In a regime where $T_S \gg T_{\rm CMB}$ and $x_H = 1$ then δT_B will be an unbiased tracer of the density field. At all other times the effects of astrophysics must be modelled and removed or somehow avoided. We will return to a discussion of this point in §7 as this is a critical point.

In this section, we take the optimistic view that there will a regime in which $\delta T_b \propto (1+\delta)$ so that the 21cm signal provides a clean measurement of the density field. This approach enables us to evaluate the best case scenario for SKA in measuring cosmological parameters. By comparing this to galaxy surveys we get a sense of how competitive SKA could be, if astrophysics could be overcome.

The sensitivity of a radio interferometer to the 21cm power spectrum has been well studied [**?**, **?**, **?**] and we follow the same approach here. The variance of a 21 cm power spectrum estimate for a single **k**-mode with line of sight component $k_{||} = \mu k$ is given by [**?**]:

$$\sigma_P^2(k,\mu) = \frac{1}{N_{\rm field}}\left[\bar{T}_b^2 P_{21}(k,\mu) + T_{\rm sys}^2 \frac{1}{Bt_{\rm int}} \frac{D^2 \Delta D}{n(k_\perp)} \left(\frac{\lambda^2}{A_e}\right)^2\right]^2 . \tag{2.2}$$

The first term on the right-hand-side of the above expression provides the contribution from sample variance, while the second describes the thermal noise of the radio telescope. The thermal noise depends upon the system temperature $T_{\rm sys}$, the survey bandwidth B, the total observing time $t_{\rm int}$, the conformal distance $D(z)$ to the center of the survey at redshift z, the depth of the survey ΔD, the observed wavelength λ, and the effective collecting area of each antennae tile A_e. The effect of the configuration of the antennae is encoded in the number density of baselines $n_\perp(k)$ that observe a mode with transverse wavenumber $k_\perp$ [**?**]. Observing a number of fields $N_{\rm field}$ further reduces the variance.

Estimates of the error on a power spectrum measurement are calculated using the Fisher matrix formalism, so that the $1-\sigma$ errors on the model parameter λ_i are $(\mathbf{F}_{ij}^{-1})^{1/2}$, where

$$F_{ij} = \sum_\mu \frac{\varepsilon k^3 V_{\rm survey}}{4\pi^2} \frac{1}{\sigma_P^2(k,\mu)} \frac{\partial P_{T_b}}{\partial \lambda_i} \frac{\partial P_{T_b}}{\partial \lambda_j}. \tag{2.3}$$

In this equation, $V_{\rm survey} = D^2 \Delta D(\lambda^2/A_e)$ denotes the effective survey volume of our radio telescopes and we assume wavenumber bins of width $\Delta k = \varepsilon k$. We will be interested in the cases where $\lambda_i = \{\bar{P}_{T_b}\}$ and $\lambda_i = \{P_{\mu^0}, P_{\mu^2}, P_{\mu^4}\}$.

sensitivity plot for various experiments relative to density field

Table 1: Low-frequency radio telescopes and their parameters. We specify the number of antennae N_a, total collecting area $A_{\rm tot}$, bandwidth B, and total integration time $t_{\rm int}$ for each instrument. These values are fixed at $z =$?? and extrapolated to other frequencies using $A_{\rm tot} = N_{\rm ant} N_{\rm dip} A_{\rm dip}$ with the number of antennae per station $N_{\rm dip} = 289$ and $A_{\rm dip} = \min(\lambda^2/3, 3.2\,{\rm m}^2)$.

Array	N_a	$A_{\rm tot}(10^3\,{\rm m}^2)$	B (MHz)	$t_{\rm int}$ (hr)	$R_{\rm min}(m)$	$R_{\rm max}(km)$
MWA	112	1.6	8	1000	4	0.75
LOFAR Core	48	38.6	8	1000	100	1.5
HERA	331	50.0	8	1000	14.3	0.3
SKA0	850×0.5	290×0.5	8	1000	35	2
SKA1	850	290	8	1000	35	2
SKA2	850×4	290×4	8	1000	35	2

We first illustrate the sensitivity of different iterations of SKA in Figure 2, where we take the parameters in Table 1 for SKA0 - with 50% of the SKA1 baseline collecting area, SKA1, and SKA2 - with x4 the collecting area of SKA1. For each of these we assume a filled core followed by r^{-2} distribution out to a maximum radius $R_{\rm max}$. HERA is assumed to have a uniform antennae distribution.

SKA1 has 911 stations total with 899 in the core and 650 stations within a radius of 1km accounting for 75% of the total number of stations and collecting area. Physical station size is 35m. Stations have 289 antennae with antennae area $A_e = \lambda^2/3$ giving $3.2m^2$ at 110MHz. At lower frequencies the array is densely packed and has constant collecting area, at higher frequencies the array becomes sparse.

Figure 2 illustrates a few key points governing parameter constraints. Here we have eliminated modes whose wavelength exceeds the instrument bandwidth removing sensitivity to the largest

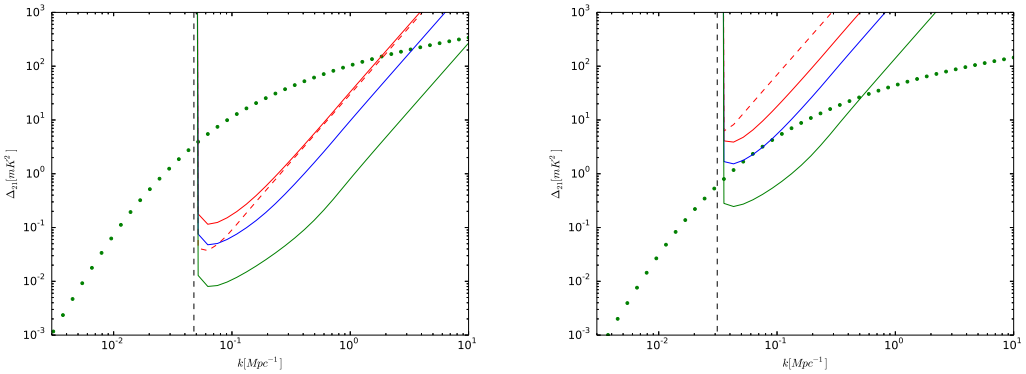

Figure 2: Sensitivity plots of HERA (red dashed curve), SKA0 (red), SKA1 (blue), and SKA2 (green). Dotted curve shows the predicted 21cm signal from the density field alone assuming $x_H = 1$ and $T_S \gg T_{\rm CMB}$. Vertical black dashed line indicates the smallest wavenumber probed in the frequency direction $k = 2\pi/y$, which may limit foreground removal. *Left panel:* $z = 8$ *Right panel:* $z = 20$.

physical scales (smallest k modes). At $z = 8$, SKA0 is directly comparable in sensitivity to the proposed HERA experiment [**?**], which is more centrally concentrated to compensate for its small number of stations. By $z = 20$ the amplitude of the 21 cm signal is too small to be detected by SKA1 *if we assume* $T_S \gg T_\gamma$. Detection of the 21cm signal at $z \gtrsim 20$ with SKA1 is dependent upon a strong 21cm absorption signal that boosts the amplitude of the 21cm power spectrum. Unfortunately, it seems likely that during the absorption regime the details and spatial variation of the spin temperature will matter and complicated getting at cosmology.

concept of effective volume and how SKA compares to various galaxy surveys

The key parameters for determining cosmological parameters are the effective volume probed and the minimum wavenumber probed $k_{\rm min}$ where modes can still be assumed to be linear. SKA has a significant advantage over galaxy surveys as more modes are still in the linear regime at $z > 6$. We set $k_{\rm min} = 2{\rm Mpc}^{-1}$ **justify or do better**

Figure 3: Effective volume and comparison of SKA to Euclid

Comment on higher redshift giving other advantages, eg isocurvature, where effects become smaller deeper into matter dominated regime.

Table 2 shows the cosmological parameters obtained with the listed experimental performances.

Table 2: Fiducial parameter values and $1-\sigma$ experimental uncertainties for cosmological parameters. Dashes indicate parameters not relevant for that experiment; ∞ indicates parameters that are relevant, but not constrained.

	$\Omega_m h^2$	$\Omega_b h^2$	Ω_Λ	w	n_s	A_s^2	τ	Y_{He}	M_ν
Fiducial	0.147	0.023	0.7	-1	0.95	26.6	0.1	0.24	0.3
SDSS	0.456	0.083	0.117	1.21	0.503	∞	...	...	

2.1 Core cosmological parameters

2.2 Inflationary parameters

2.3 Neutrino mass

3. Constraining new physics from heating

The 21cm signal probes both the ionization and thermal state of the IGM. Although we do not know the precise timing and evolution of the signal, empirical scaling relations based on local star-forming galaxies (e.g. Mineo+2012) suggest that the X-rays from early galaxies heat the IGM to temperatures above the CMB before the bulk of reionization (e.g. Furlaneto 2006; §2.1 in McQuinn & OÕLeary 2012). This marks the transition of the 21cm signal from absorption to emission, with large-scale fluctuations in gas temperature likely driving the 21cm power to its largest amplitude (e.g. Pritchard & Furlanetto 2007; Baek+2010). The epoch of IGM heating is a powerful probe of the high-energy processes in the early Universe, with could have both astrophysical and cosmological origins. Both can tells us about the nature of dark matter (DM).

In order to explain the apparent deficiencies of CDM on small (sub-Mpc) scales, Warm Dark Matter (WDM) models have recently gained in popularity. In these models, DM is assumed to consist of smaller mass particles, $\sim$ keV, such as the sterile neutrino or gravitino. The increased particle free-streaming and velocity dispersion (acting as a sort of effective pressure), can dramatically suppress structures on small-scales. This suppression is even more obvious in the early Universe, where typical halos hosting galaxies were much smaller, and larger structures did not have time to fragment. Current astrophysical lower limits on the WDM particle range from $m_x \gtrsim$ 1Ð3 keV (assuming a thermal relic relativistic at decoupling), with various degrees of astrophysical degeneracy (e.g. [**?**, **?**, **?**, **?**])

The resulting dearth of galaxies in the early Universe means that the astrophysical epochs in the 21cm signal were delayed. The challenge as always will be to disentangle the cosmological impact from astrophysical uncertainties, such an a lower than expected star formation efficiency in CDM. Since the fractional suppression of structure increases with redshift, this becomes much easier with the first galaxies observable with the SKA. For example, we only need to understand the astrophysics of the first galaxies to an order of magnitude in order to improve on current m_X constraints (Sitwell+ http://adsabs.harvard.edu/abs/2014MNRAS.438.2664S) Moreover, even if the star-formation efficiency in CDM is allowed to vary in order to mimic the mean 21cm evolution in WDM models, the signal will still not be completely degenerate (see Fig. 4a). This is due to the fact that the galaxies driving the 21cm evolution in WDM should reside in higher mass, more

rapidly evolving halos, than those in CDM. The increased bias of such halos results in a larger 21cm fluctuations (see Fig. 4a).

The heating of the IGM could also have a cosmological component. In particular, annihilations of dark matter particles in the $\sim$ 10 GeV mass range (motivated by recent results from indirect experiments; e.g. [**?**, **?**, **?**]) could provide a dominant source of heat, before the birth of the first galaxies. Driven by the evolution of $\sim M.$ structures, several order os magnitude smaller than those hosting galaxies, heating is expected to be much slower in such models, resulting in a smaller brightness temperature gradient $d\delta Tb/d? \sim 4mKMHz^{-1}$ in the range $? \sim 60?80$ MHz (valdes+2013). Moreover, DM annihilations would heat the IGM quite uniformly, which is not the case for heating driven by astrophysical sources residing in early galaxies. The resulting lack of temperature fluctuations (see Fig. 4b) would result in dramatic drop in 21cm power during heating, which would be easy to identify with the SKA (Evoli+ in prep). Furthermore, the ensuing rise in 21cm power when the galaxies start contributing to heating the IGM should occur *when the IGM is already in emission*. The later is a qualitatively robust signature of DM annihilation heating, easily obtainable with the SKA.

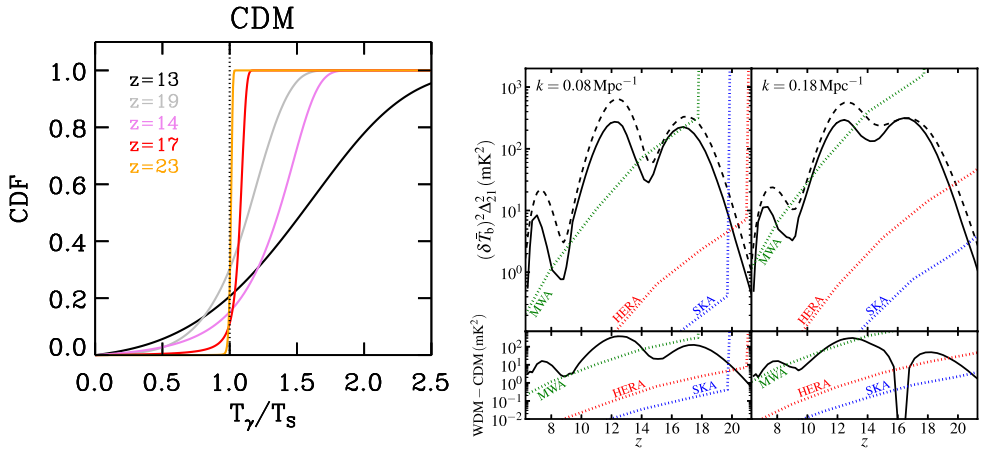

Figure 4: *Right panel:* Evolution of the power spectrum of ?Tb for WDM with $m_X = 2$ keV. The top panels show power spectra at k = 0.08, 0.18 Mpc?1 for WDM (dashed) and the CDM model (solid). CDM models have f?(z) (star-formation efficiency) chosen to reproduce the global 21-cm signal found for the respective WDM model. The bottom panels show the difference in the power spectrum between WDM and CDM models. Dotted curves show forecasts for the 1? power spectrum thermal noise as computed in Mesinger et al. (2013a) assuming 2000 h of observation time. The dotted green, blue and red curves are the forecasts for the MWA, SKA and HERA, respectively. This figure is from Sitwell+2014. CDFs of T?/TS corresponding to the fiducial and extreme astrophysical X-ray heating (black and gray curves respectively) from Mesinger+2013. The colored curves correspond to models in which 10 GeV DM annihilations are also accounted for (in addition to fiducial astrophysical heating), with varying relative contribution. The curves correspond to the redshift for which Ts ? TCMB. Figure is from Evoli, mesinger, Ferrara, in prep.

4. Fundamental physics from modifications to the source population

5. Bulk flows

6. Cosmic shear and the EoR

It is possible that the EoR signal could be used to measure weak gravitational lensing. In [2] and [3] it was shown that if the EoR is at redshift $z \sim 8$ or later, a large radio telescope such as the SKA could measure the lensing convergence power spectrum. However a very large $f_{\rm sky}$ and a very compact low frequency array was assumed by those authors. Here the calculation is repeated with parameters that are more consistent with current SKA plans. The current plans for a 25 square degree survey with SKA_Low will preclude measuring cosmological parameters through their effects on the weak lensing power-spectrum because of large sample variance. (This is not true of the SKA_Mid at lower redshift where the survey area will be much larger. See section *** for more details.) It still might be possible to map the lensing convergence within the 25 square degree EoR survey area. This would allow us to actually "see" the distribution of dark matter in a typical region of the sky, something that is only possible with galaxy lensing around very atypical, large galaxy clusters.

The previously mentioned authors extended the Fourier-space quadratic estimator technique, which was first developed in [4] for CMB lensing observations to three dimensional observables, i.e. the 21 cm intensity field $I(\theta, z)$. The convergence estimator and the corresponding lensing reconstruction noise are calculated assuming that the temperature (brightness) distribution is Gaussian. This will not be strictly true during the EoR, but serves as a reasonable approximation for these purposes. Note that the lensing reconstructions noise contains the thermal noise of the telescope which is calculated using the formula

$$C_\ell^{\rm N} = \frac{(2\pi)^3 T_{\rm sys}^2}{\Delta\nu t_{\rm obs} f_{\rm cover}^2 \ell_{\rm max}(\nu)^2}\,, \tag{6.1}$$

where the system temperature $T_{\rm sys}$ at high redshifts is dominated by galactic synchrotron radiation, $\Delta\nu$ is the chosen frequency window, $t_{\rm obs}$ the total observation time, $D_{\rm tel}$ the diameter (maximum baseline) of the core array and $\ell_{\rm max}(\lambda) = 2\pi D_{\rm tel}/\lambda$ is the highest multipole that can be measured by the array at frequency ν (wavelength λ). $f_{\rm cover}$ is the total collecting area of the core array $A_{\rm coll}$ divided by $\pi(D_{\rm tel}/2)^2$. For SKA_Low we can consider a $1,000$ hr observation time and we choose $\Delta\nu = 10\,$MHz, but with multiple bands that can be stacked to reduce the noise.

We assuming the SKA1 Baseline Design [5] parameters of $A_{\rm coll} \simeq 0.4\,{\rm km}^2$ with maximum baseline $D_{\rm tel} = 6\,$km and a more compact configuration of $A_{\rm coll} = 0.75\,{\rm km}^2$, $D_{\rm tel} = 2\,$km. The estimated lensing noise is shown in Figure 5 along with the estimated signal. Here C_L is the displacement field power spectrum and N_L the lensing reconstruction noise assuming a reionization fraction $f_{\rm HI} = 1$ at the source redshift $z_s = 8$.

These results show that it might be possible to map the lensing signal over a range of angular scales. This measurement would greatly benefit from a more compact array and/or the large collecting area that will come with Phase 2. The weak lensing power spectrum can be better measured for redshifts after reionization using SKAMid and the same 21 cm intensity mapping technique discussed, but over a much larger area of sky [6].

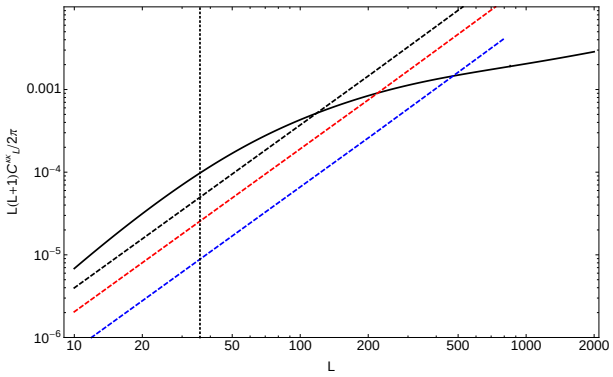

Figure 5: The lensing displacement field power spectrum, C_L, for sources at $z = 8$ is shown as a solid black line and lensing reconstruction noise N_L as dashed lines. The black dashed curve is for the Baseline Design with 20 5 MHz frequency bins around $z = 8$ spanning the redshift range $z = 6 - 12$. The blue line is for the more compact array ($D_{\rm tel} = 2$km) and the same frequency bins. The red line is the same as the blue but with 10 5 MHz frequency bins instead of 20, spanning the redshift range $z = 7 - 10$. The vertical line is approximately the lowest L accessible with a 5-by-5 degree field. Where the noise curves are below C_L typical fluctuations in the lensing deflection should be recoverable in a map.

7. Separating “gastrophysics" and cosmology

The key challenge for extracting fundamental physics from the 21cm signal will be separating the effects of cosmology from “gastrophysics". A number of avenues have been studied in the literature, which broadly separate into (1) avoidance and (2) modelling. In the absence of a clearly defined window where $T_S \gg T_{\rm CMB}$ and $x_H = 1$ it might still be possible to avoid astrophysics via the angular dependence of the power spectrum induced by redshift space distortions. Focussing on the $P_{\mu^4} \approx P_\delta$ part could lead to clean cosmological measurements. Obtaining precision cosmology this way is hard and the literature suggests little improvement over Planck is possible [7, 8]. Figure 6 shows predicted errors bars for SKA1 on the P_{μ^2} and P_{μ^4} parts of the power spectrum. A detection is possible with reasonable sensitivity at wavenumbers $k = 0.1 - 1\,{\rm Mpc}^{-1}$.

Information in P_{μ^2} is likely to help with modelling of the astrophysics.

Compared with the CMB our theoretical understanding of the 21cm signal during reionization is poor. Predictions for the 21cm power spectrum do not exist at the same level of precision as the cosmology. Nonetheless, we expect the contribution of astrophysics to be relatively broad band and determined by extra power about a characteristic scale, eg the bubble size during reionization.

8. Paths to cosmology with Phase 1 and Phase 2

9. Miscellaneous?

References

[1] S. R. Furlanetto, S. P. Oh, and E. Pierpaoli. Effects of dark matter decay and annihilation on the high-redshift 21cm background. *PRD*, 74(10):103502, November 2006.

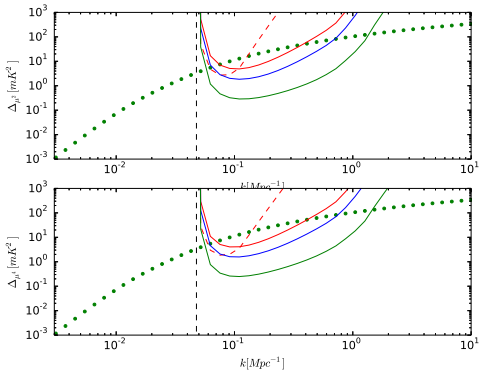

Figure 6: Sensitivity plots on P_{μ^2} and P_{μ^4} for HERA (red dashed curve), SKA0 (red), SKA1 (blue), and SKA2 (green). Dotted curve shows the predicted 21cm signal from the density field alone assuming $x_H = 1$ and $T_S \gg T_{\rm CMB}$. Vertical black dashed line indicates the smallest wavenumber probed in the frequency direction $k = 2\pi/y$, which may limit foreground removal. *Left panel:* $z = 8$ *Right panel:* $z = 20$.

[2] O. Zahn and M. Zaldarriaga. Lensing Reconstruction Using Redshifted 21 Centimeter Fluctuations. *ApJ*, 653:922–935, December 2006.

[3] R. B. Metcalf and S. D. M. White. Cosmological information in the gravitational lensing of pregalactic HI. *MNRAS*, 394:704–714, April 2009.

[4] W. Hu. Mapping the Dark Matter through the Cosmic Microwave Background Damping Tail. *ApJ*, 557:L79–L83, August 2001.

[5] P. Dewdney. SKA1 System Baseline Design. *SKA Project Documents*, pages 1–98, 2013.

[6] A. Pourtsidou and R. B. Metcalf. Weak lensing with 21 cm intensity mapping at z $\sim$ 2-3. *MNRAS*, 439:L36–L40, March 2014.

[7] M. McQuinn, O. Zahn, M. Zaldarriaga, L. Hernquist, and S. R. Furlanetto. Cosmological Parameter Estimation Using 21 cm Radiation from the Epoch of Reionization. *ApJ*, 653:815–834, December 2006.

[8] Y. Mao, M. Tegmark, M. McQuinn, M. Zaldarriaga, and O. Zahn. How accurately can 21cm tomography constrain cosmology? *PRD*, 78(2):023529, July 2008.